Supporting Information

One-step and template-free preparation of hierarchical porous carbons with high capacitive performance

Jin Zhou*, Zhongshen Zhang, Zhaohui Li, Tingting Zhu, and Shuping Zhuo*

School of Chemical Engineering, Shandong University of Technology, Zibo 255049, P. R. China. Tel. /fax: +86 533 2781664

Table of Contents

Fig. S1 Photographic pictures of the hydrogel and xerogel

Fig. S2 SEM images (a, b) HPC-6, (c) HPC-7, (d) HPC-8, (e, f, g) HPC-9 and (h) HPC-10

Fig. S3 TEM images (a) HPC-6, (b) HPC-7, (c) HPC-8, (d) HPC-9 and (e, f) HPC-10

Fig. S4 Porosity analysis of HPC-*x* (a) nitrogen sorption isotherms, (b, c) NLDFT pore size distribution calculated from N_2 adsorption isotherms, (d) NLDFT micropore size distribution calculated from CO_2 adsorpiton isotherms

Fig. S5 (a) N_2 sorption isotherms and (b) pore size distribution of direct-dried xerogels

Fig. S6 (a) N_2 sorption isotherms and (b) pore size distributions of HPC carbon prepared at 900^{o}C

Fig. S7 (a) Galvanostatic charge/discharge curves at different current density, (b) volumetric capacitance of HPC-9d and CMK-3 in KOH and organic electrolytes

Fig. S8 Specific capacitances of HPC carbon prepared at 900 °C in KOH electrolyte

Fig. S9 normalized imaginary capacitance vs. alternative current frequency

Fig. S10 (a) CV curves of HPC-9d at different scan rate and (b) galvanostatic charge/discharge curves of HPC-9d at different current density in $TEABF_4$/AN electrolyte

Table S1 Texture properties of samples

Table S2 Values of I_D/I_G for the prepared carbon materials in this work

Table S3 Specific capacitance at 0.20 A g^{-1} and the time constant in KOH electrolyte

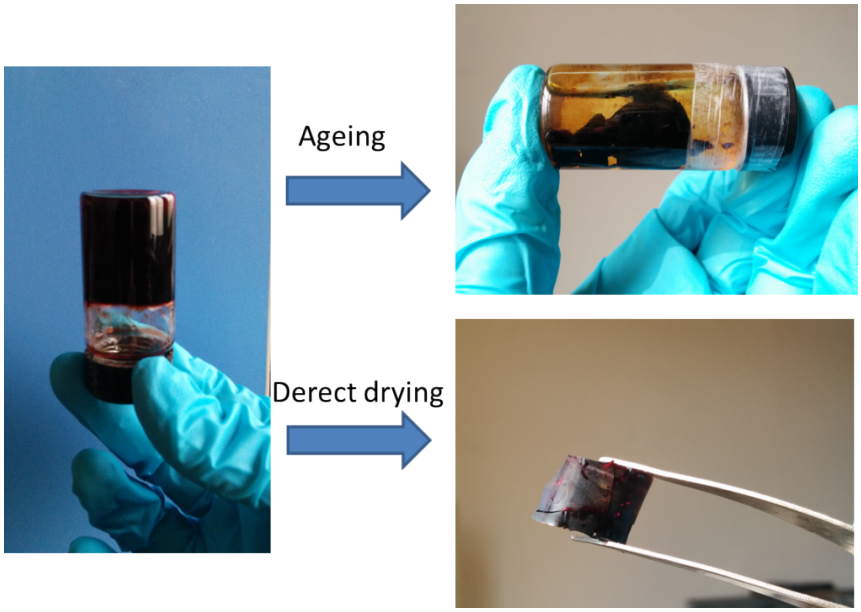

Fig. S1 Photographic pictures of the hydrogel and xerogel

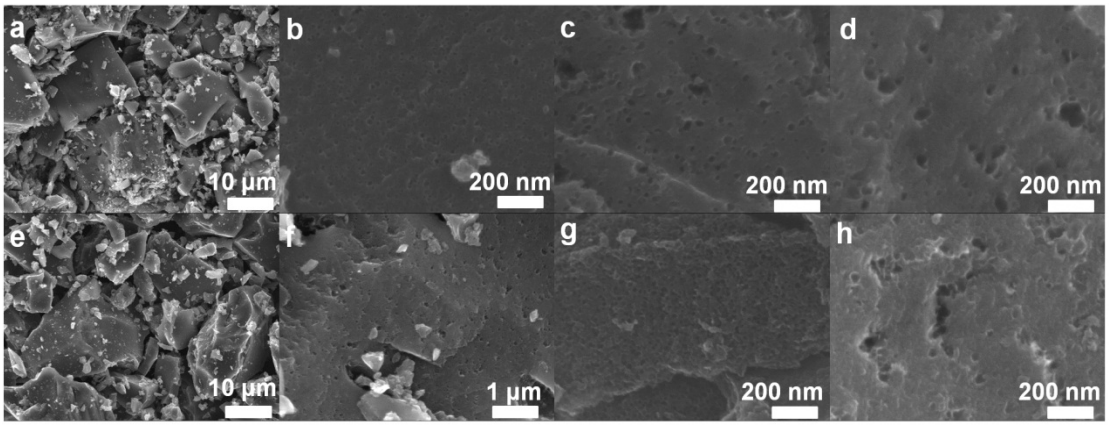

Fig. S2 SEM images (a, b) HPC-6, (c) HPC-7, (d) HPC-8, (e, f, g) HPC-9 and (h) HPC-10

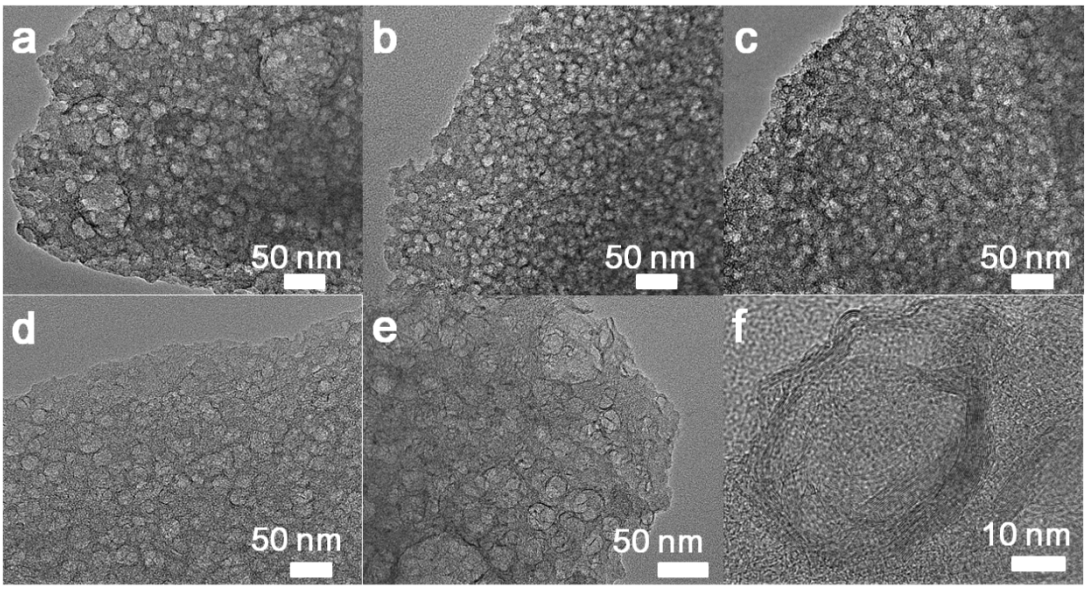

Fig. S3 TEM images (a) HPC-6, (b) HPC-7, (c) HPC-8, (d) HPC-9 and (e, f) HPC-10

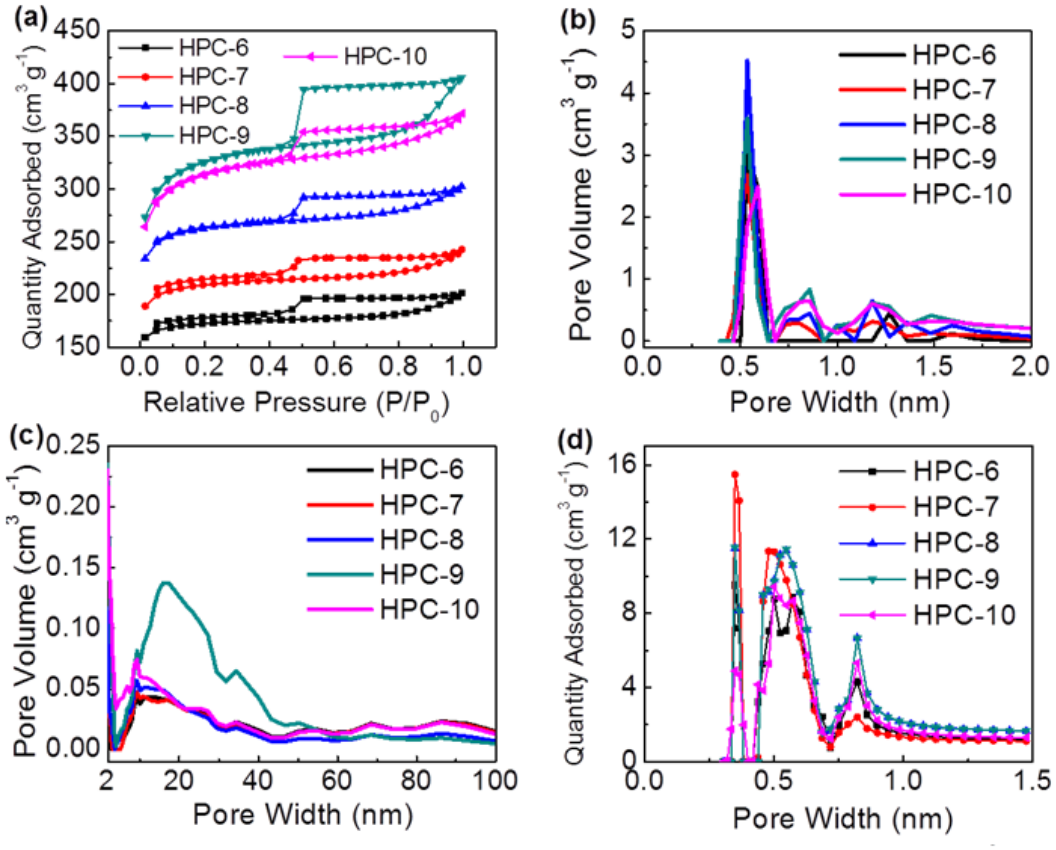

Fig. S4 Porosity analysis of HPC-*x* (a) nitrogen sorption isotherms, (b, c) NLDFT pore size distribution calculated from N_2 adsorption isotherms, (d) NLDFT micropore size distribution calculated from CO_2 adsorpiton isotherms

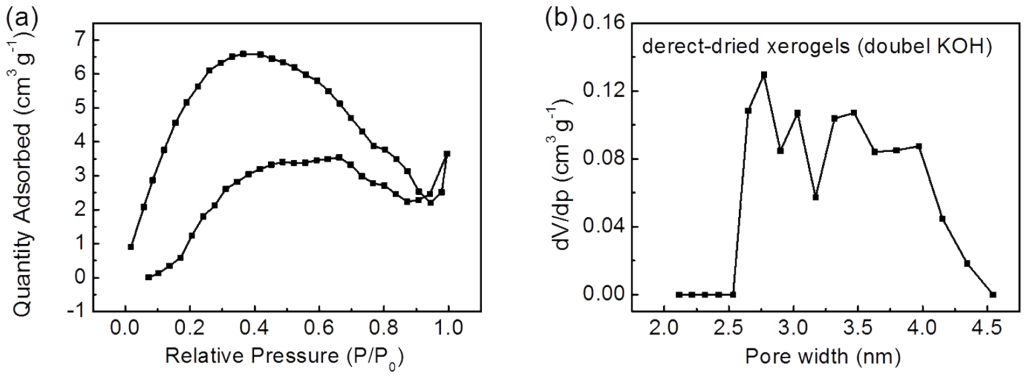

Fig. S5 (a) N_2 sorption isotherms and (b) pore size distribution of direct-dried xerogels

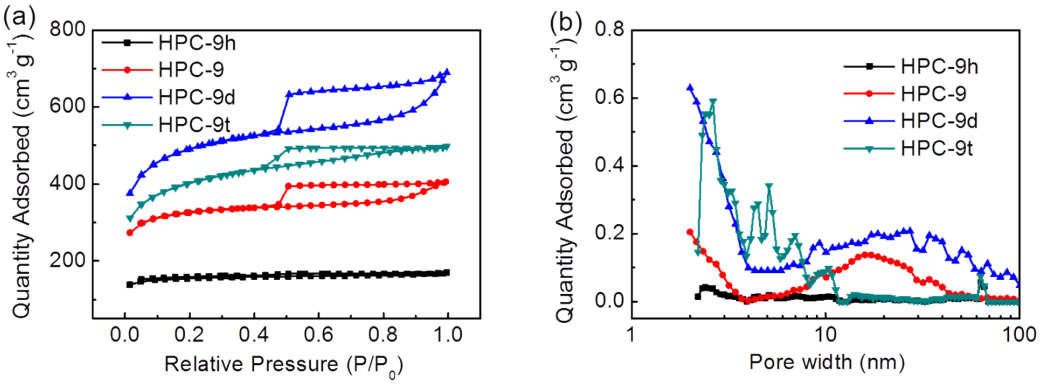

Fig. S6 (a) N_2 sorption isotherms and (b) pore size distributions of HPC carbon prepared at 900^{o}C

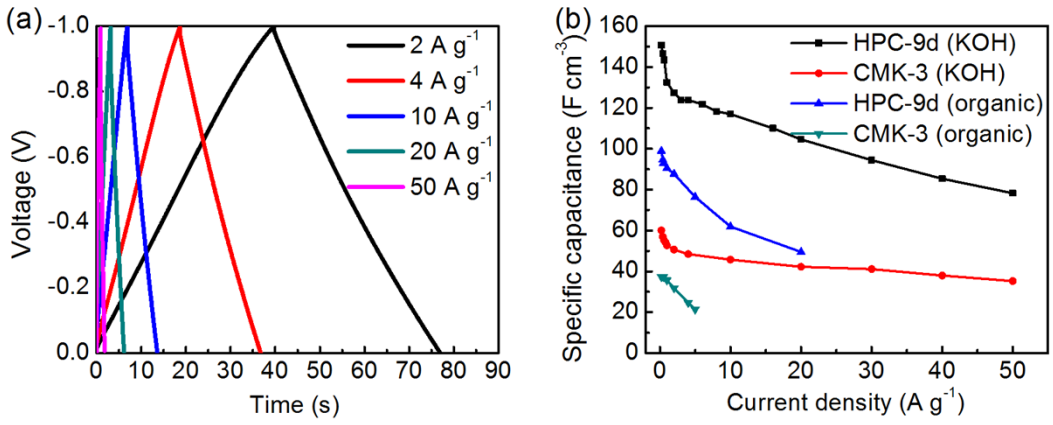

Fig. S7 (a) Galvanostatic charge/discharge curves at different current density, (b) volumetric capacitance of HPC-9d and CMK-3 in KOH and organic electrolytes

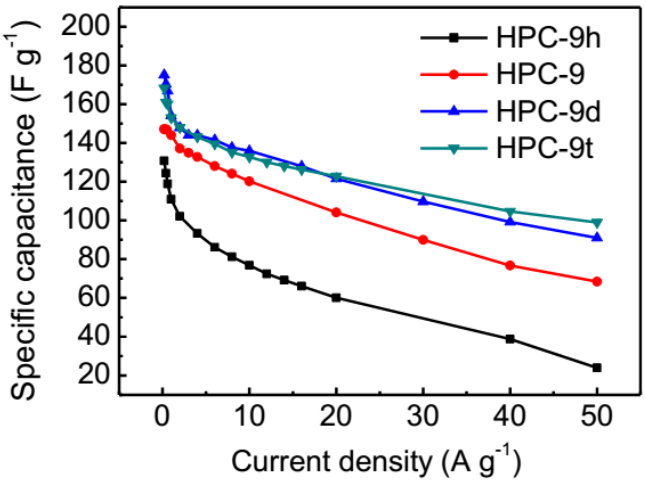

Fig. S8 Specific capacitances of HPC carbon prepared at 900 °C in KOH electrolyte

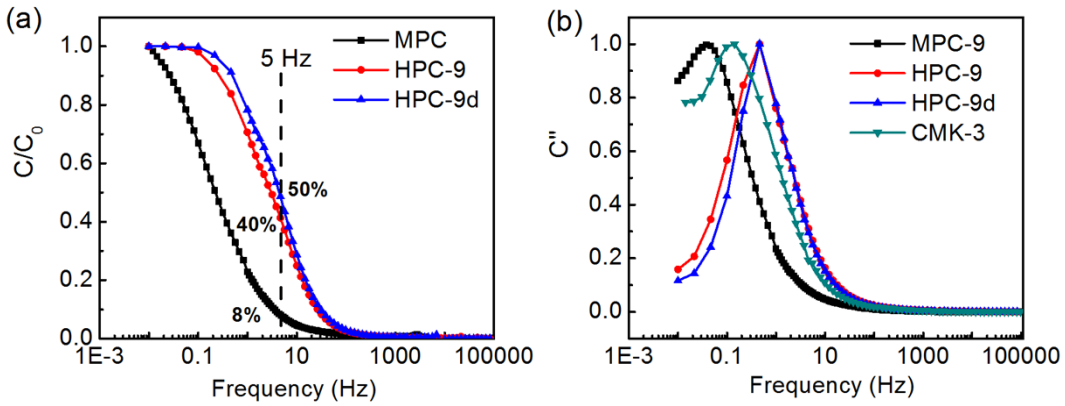

Fig. S9 normalized imaginary capacitance vs. alternative current frequency

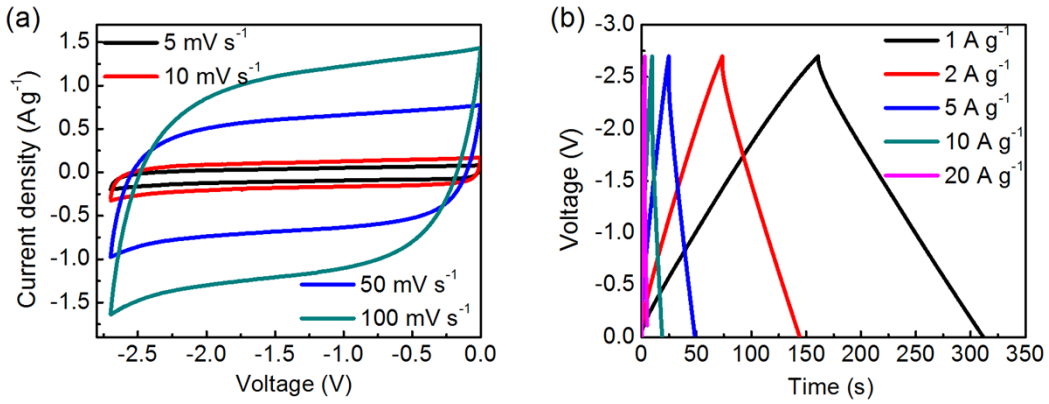

Fig. S10 (a) CV curves of HPC-9d at different scan rate and (b) galvanostatic charge/discharge curves of HPC-9d at different current density in $TEABF_4$/AN electrolyte

Table S1 Texture properties of samples

Sample	S_{BET} (m^2 g^{-1})	V_T (cm^3 g^{-1})	V_{meso} (cm^3 g^{-1})	V_{micro} (cm^3 g^{-1})
HPC-9h	473	0.26	0.04	0.22
HPC-9	1007	0.62	0.16	0.46
HPC-9d	1549	0.81	0.17	0.61
HPC-9t	1387	0.77	0.29	0.48

Table S2 Values of I_D/I_G for the prepared carbon materials in this work

Sample	HPC-6	HPC-7	HPC-8	HPC-9	HPC-10	HPC-9d	MPC-9
I_D/I_G	0.80	0.82	0.84	0.85	0.85	0.86	0.83

Table S3 Specific capacitance at 0.20 A g^{-1} and the time constant in KOH electrolyte

Samples	C_{KOH} (F g^{-1})	$C_{Organic}$ (F g^{-1})	τ
MPC-9	174.4	1.9	3.95
HPC-9	147.2	38.0	0.36
HPC-9d	175.2	115.0	0.33
CMK-3	126.6	78.6	1.17